



FUSION EN

ORNL/Sub-79/21453/4

aj.24

60 GHz GYROTRON DEVELOPMENT PROGRAM

J. F. Shively, T. J. Grant, D. S. Stone,
R. S. Symons and G. E. Wendell

Quarterly Report No. 4
April through June 1980

Prepared for:

OAK RIDGE NATIONAL LABORATORY
OAK RIDGE, TENNESSEE 37830

Operated by:

UNION CARBIDE CORPORATION
FOR THE DEPARTMENT OF ENERGY

CONTRACT NO. W-7405-ENG-26

Varian Associates, Inc.
Palo Alto Microwave Tube Division
611 Hansen Way
Palo Alto, California 94303

60 GHz GYROTRON DEVELOPMENT PROGRAM

J.F. Shively, T.J. Grant, D.S. Stone, R.S. Symons and G.E. Wendell

Quarterly Report No. 4
April through June 1980

Prepared for:
Oak Ridge National Laboratory
Oak Ridge, Tennessee 37830

Operated by:
Union Carbide Corporation
for the
Department of Energy
Contract No. W-7405-eng-26

Varian Associates, Inc.
Palo Alto Microwave Tube Division
611 Hansen Way
Palo Alto, CA 94303

ABSTRACT

The objective of this program is to develop a microwave oscillator capable of producing 200 kW of CW output power at 60 GHz. The use of cyclotron resonance interaction is being pursued.

The design and early procurement and construction phases of this program are discussed.

TABLE OF CONTENTS

<u>Section</u>		<u>Page</u>
I.	INTRODUCTION	1
II.	ELECTRON BEAM	3
III.	THE ELECTRON GUN	5
IV.	SUPERCONDUCTING SOLENOID MAGNET	6
V.	INTERACTION CIRCUIT	9
VI.	OUTPUT/COLLECTOR	13
	A. Definition of VTWR	13
	B. VTWR's in Cylindrical Waveguide	15
	C. Mode Bunches	15
	D. Guide Factors	16
VII.	WINDOW	20
VIII.	MECHANICAL DESIGN	24
IX.	COMPONENTS	27
X.	TUBE ASSEMBLY	28
XI.	PROGRAM SCHEDULE AND PLANS	29
XII.	REFERENCES	35

LIST OF ILLUSTRATIONS

<u>Figure</u>		<u>Page</u>
1.	Electron Trajectory Calculations for Experimental Pulsed Gyrotron Collector	4
2.	Outline VYW-8060 Coil and Dewar Assembly	8
3.	Azimuthal Electric Field Squared for the TE ₀₂₁ Oscillator Cavity in Arbitrary Units vs Normalized Axial Position, Z/a, At the Fixed Radius Corresponding to the First Radial Maximum of the Electric Field	11
4.	Computed VSWR for a Single-disc Beryllia Window	21
5.	Computed VSWR for an FC-75 Face-Cooled Alumina Double-disc Window	22
6.	Computed VSWR for an FC-75 Face-cooled Beryllia Double-disc Window	23
7.	Milestone Chart and Status Report	30

LIST OF TABLES

<u>Table</u>		<u>Page</u>
I	Guide factors for circular electric mode bunches ...	17
II	One-half beat wavelengths	18
III	VTWR measurement intervals	18

I. INTRODUCTION

The current objective of this program is to develop a microwave oscillator capable of producing 200 kW of CW output power at 60 GHz. Tunability or bandwidth is not considered an important parameter in the design, but efficiency is. Mode purity in the output waveguide is not a requirement for the device, but the circular electric mode is considered desirable because of its low loss properties.

With these objectives in mind, an approach based on cyclotron resonance interaction between an electron beam and microwave fields is being pursued. The detailed arguments leading to this approach are contained in the final report of a preceding study program.¹ The device configurations of particular interest, called gyrotrons, have been discussed in recent literature.²⁻⁶ They employ a hollow electron beam interacting with cylindrical resonators of the TE_{0m1} class.

The optimum beam for the cyclotron resonance interaction is one in which the electrons have most of their energy in velocities perpendicular to the axial magnetic field. Another requirement is that the spread in the axial components of the electron velocities be as small as possible. Electrons which have different axial velocities will not interact efficiently.

The approach chosen to generate the beam is a magnetron type of gun as is used on the 28 GHz gyrotron, also developed for Oak Ridge National Laboratory.^{7,8} With this type of gun the shaping of the magnetic field in the gun region becomes quite important.

Construction of the first experimental 60 GHz gyrotron has been started. Electron gun parts are on order. A purchase order has been placed with Magnetic Corporation of America for the superconducting solenoid magnet. Assembly of the anode and oscillator cavity assembly has also been

started. A cold test model of the CW collector has been constructed and most of the cold test equipment has been received, as well as the microwave window parts. At present, the limiting item appears to be modification of the test set.

II. ELECTRON BEAM

A computer simulation of the electron beam was done for the pulsed tube collector design.

Twenty-four trajectories were calculated starting from the interaction circuit with eight electrons arranged about each of three orbit centers. Because of program size limitations, four axial collector segments were required in the calculation to reach the area where interception occurs.

The calculations were made using the fringing field of the superconducting magnet system with no additional coils in the collector region for field shaping.

Figure 1 shows the plots of the trajectories in the region 20.5 to 50.0 inches from the center of the interaction circuit. The first trajectory intercepted approximately 10 inches beyond the lower collector seal. The beam loading is spread over an axial length of approximately 2 feet.

An estimate of the peak power density on the collector walls will require more detailed trajectory simulation runs.

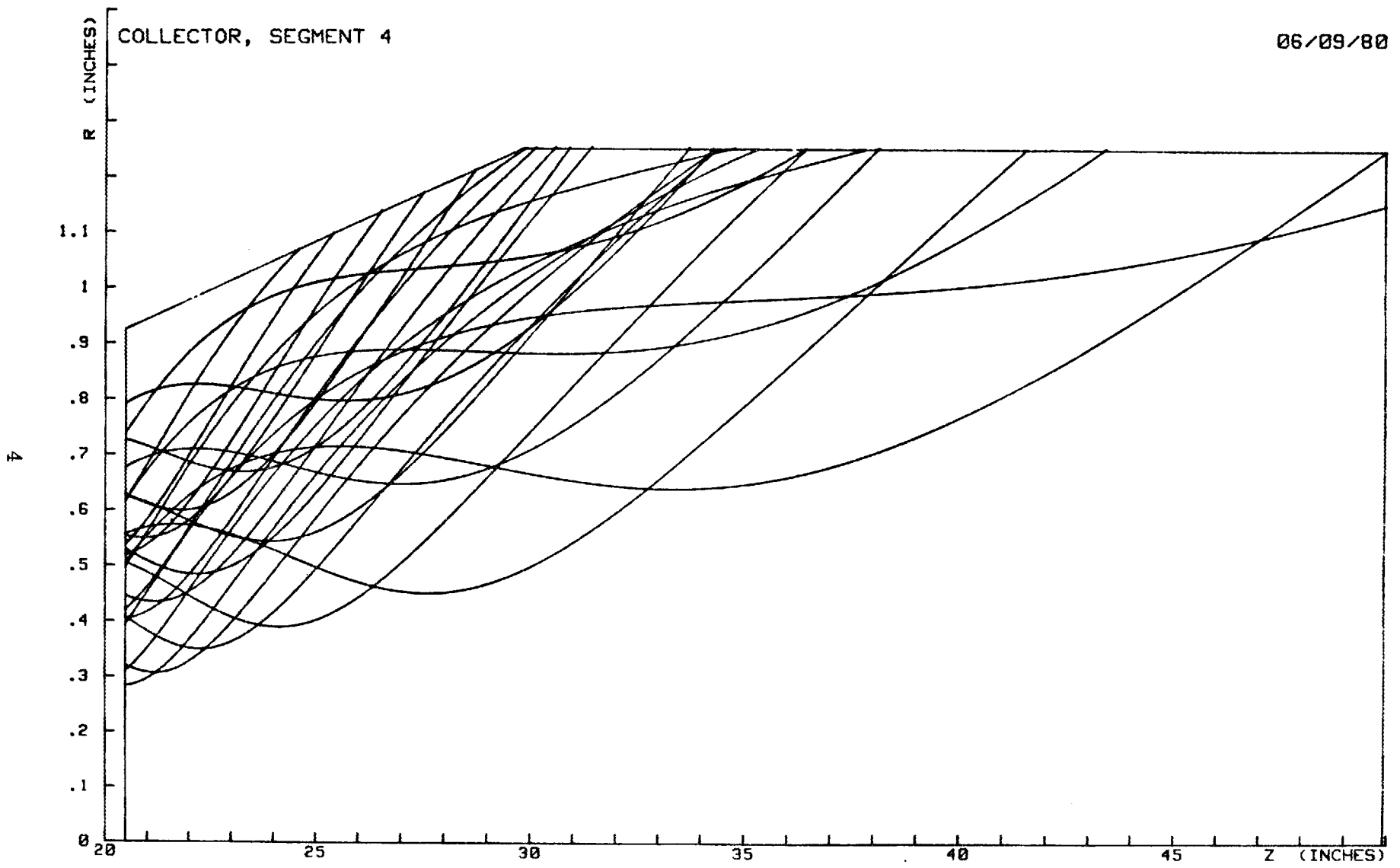


**FIGURE 1. ELECTRON TRAJECTORY CALCULATIONS FOR
EXPERIMENTAL PULSED GYROTRON COLLECTOR**

III. THE ELECTRON GUN

The procurement cycle for the electron gun is in process. All the parts were ordered prior to the end of the quarter with the majority having a confirmed delivery date of no later than July 31. The delivery date on several critical parts, including the ceramic heater retainer rings had not been confirmed; however, confirmation dates were being expedited by Varian's Production Control Group.

Tooling for drawn parts (e.g., heat shields and seal rings) and fixtures for jiggling during gun construction were designed and ordered during the quarter. Because of the exceptionally long delivery dates quoted by outside vendors, the order for the tooling items was submitted to Varian's in-house engineering machine shop. Under a high priority production schedule, the tooling and fixtures will now meet the delivery date of July 31.

IV. SUPERCONDUCTING SOLENOID MAGNET

Both on-axis and off-axis axial and radial components of flux density were computed in addition to the vector potential using the Varian magnetostatic program which computes the normalized flux array for an iron-free magnet system in a form suitable for use in the Varian gun program.

The diameter of the bucking coil was increased to achieve better voltage hold off characteristics.

The design of the superconducting solenoid magnet consists of a split pair of coils for the main magnetic field and a bucking coil in the gun region for shaping the magnetic field in the vicinity of the magnetron injection gun. Two pairs of transverse trim coils are available for beam steering. The main coils and bucking coil will be wound on the same bobbin to ensure concentricity. The transverse coils will be outside the main coils. The entire coil assembly operates in a liquid helium bath. The liquid helium vessel is surrounded by vacuum, a liquid nitrogen temperature heat shield, vacuum and the room temperature shell.

The room temperature shell has a flange which mounts on an existing flange in the test set oil tank. The superconducting solenoid magnet will have a vertical bore. A socket to accept the tube gun will be attached to the bottom of the dewar. Leads and service ports exit the room temperature shell at a 45° angle on the outside diameter to leave the top surface of the dewar clear for possible room temperature collector coils and their supporting structure.

The thermal design will allow a day's operation after topping the liquid helium and liquid nitrogen levels. After being shut off for as long as a weekend, the liquid reservoirs will merely have to be filled, not having warmed up to a temperature requiring cooling.

A design review will be held at Magnetic Corporation of America on July 18, 1980. Delivery of the first unit is expected in November 1980.

The outline drawing of the coil and dewar assembly is shown in Figure 2.

V. INTERACTION CIRCUIT

Analytical work on the interaction circuit is continuing. We have chosen a cavity geometry which is sufficiently arbitrary that any reasonable combination of external Q, resonant frequency, and axial electric field profile may be obtained by varying the geometric parameters. The mathematical solution for the vacuum electromagnetic fields in the cavity geometry is obtained in the following manner.

An "initial value" solution for the vacuum fields, E and B, is derived for modes TE_{mnl} from a Debye potential of a form such that

$$\vec{E} = \vec{e}_z \times \nabla \pi$$

$$\vec{B} = \nabla (\vec{e}_z \cdot \nabla \pi) - \frac{\vec{e}_z \ddot{\pi}}{c^2}$$

where \vec{e}_z is the unit vector in the direction of propagation (along the z axis), c is the speed of light, and π is the Debye potential which satisfies the wave equation,

$$\square \pi = 0.$$

The boundary conditions on the components of the electromagnetic fields are:

(A) $\vec{E} \cdot \vec{e}_z = 0$ at conducting boundaries,

(B) $\vec{B}(\vec{r} = 0) \cdot \vec{e}_z \Big|_+ = \vec{B}(\vec{r} = 0) \cdot \vec{e}_z \Big|_-$ at boundaries $\perp \vec{e}_z$,

while the integrated Poynting flux is also matched at boundaries $\perp \vec{e}_z$:

(C) $\frac{1}{2} \iint (\vec{E} \times \vec{B}^*)_+ \cdot \vec{e}_z \, dA = \frac{1}{2} \iint (\vec{E} \times \vec{B}^*)_- \cdot \vec{e}_z \, dA$, and

(D) the radiative boundary condition is applied for $z \rightarrow +\infty$.

Our interaction circuit computer code, which is set in this analytical framework, can now predict the cavity electric field profile for circular electric cavity modes. Figure 3 shows a plot of the calculated electric field profile at the first radial maximum of the electric field versus axial position for the TE_{021} cavity mode. Some computational difficulties have been encountered in extending this work to noncircular electric cavity modes. Work on improving the computer code to overcome these problems is continuing. Cold testing of the interaction circuit designs is continuing with borrowed equipment.

We have modified a previous calculation (see reference 1, section 6.2) of ohmic losses in the gyrotron resonator cavity to explicitly show the dependence of cavity power dissipation in the external cavity Q . We have made several simplifying assumptions generally valid in gyrotron engineering:

- (a) the external cavity Q , Q_{EXT} , is independent of the ohmic losses in the cavity and is therefore equal to the loaded Q of the cavity, Q_L ;
- (b) the electric field profile in the cavity has an axial dependence of $\sim \sin \pi z/L$ where z is the axial position and L is the cavity length;
- (c) the cavity length is large compared to its radius, a .

With these approximations we find the result for the average power dissipation in watts/cm² in the cavity walls for a TE_{0n1} cavity:

$$\frac{dP}{dA} = \frac{Q_{EXT} P_o f^{5/2}}{\sqrt{\sigma} c^2 \left(\frac{L}{\lambda}\right) x_{in}^2} \quad (\text{cgs}) \quad (1a)$$

$$\text{with } Q_{EXT} \cong Q_L, \left(\frac{\pi a}{x_{in} L}\right)^2 \ll 1,$$

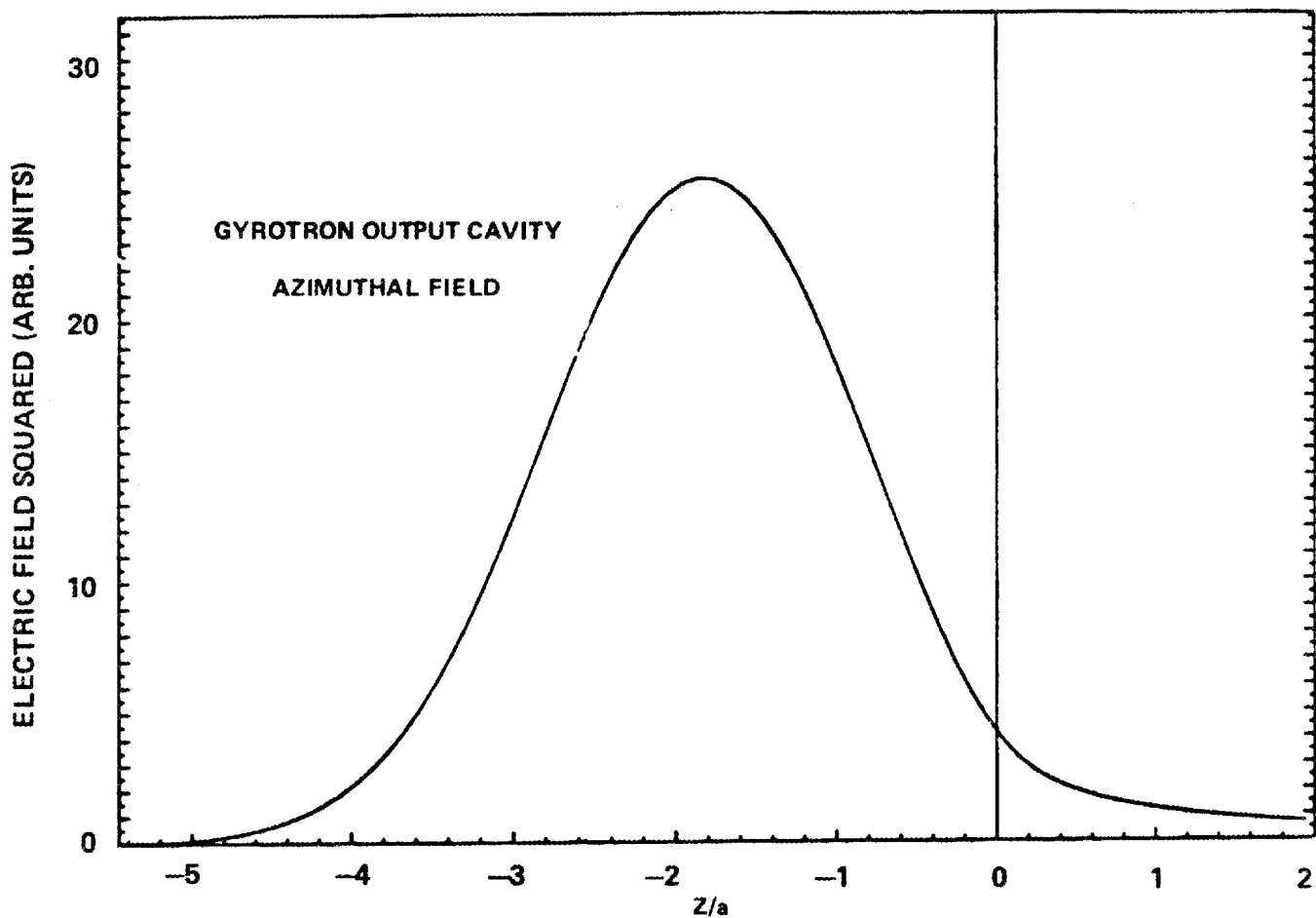


FIGURE 3. AZIMUTHAL ELECTRIC FIELD SQUARED FOR THE TE_{021} OSCILLATOR CAVITY IN ARBITRARY UNITS vs NORMALIZED AXIAL POSITION, Z/a , AT THE FIXED RADIUS CORRESPONDING TO THE FIRST RADIAL MAXIMUM OF THE ELECTRIC FIELD

where P_o is the cavity output power in watts, f is the cavity resonant frequency in hertz, c is the speed of light in cm/sec, L is the cavity length in units of $\lambda = c/f$, x_{1n} is the n^{th} positive root of the equation $J_1(x) = 0$, and σ is the rf conductivity of the cavity walls in cgs units.

For a copper cavity we find:

$$\frac{dP}{dA} \text{ (kW/cm}^2\text{)} = 4.87 \times 10^{-8} \cdot \frac{Q_{\text{EXT}} P_o \text{ (kW)} f \text{ (GHz)}^{5/2}}{\left(\frac{L}{\lambda}\right) x_{1n}^2} \quad (1b)$$

Equations 1a and 1b explicitly include the dependence of dissipation on Q_{EXT} and P_o . The strong frequency dependence of the dissipation $\sim f^{5/2}$ is clearly evident as is the advantage of using higher order TE_{on} cavity modes. For the 60 GHz, 200 kW, TE_{02} cavity mode oscillator, Equation 1b gives $dP/dA = 440 \text{ watts/cm}^2$, when we use $L/\lambda = 5$ and $Q_{\text{EXT}} = 400$.

Most of the parts required for the interaction circuit section of the tube have been received. Test brazing assemblies have been designed for investigating brazing techniques and ensuring that the brazing jigs have been properly designed. Trial fabrication of the ceramic assemblies in the anode and the load cavity had already begun at the end of the quarter.

VI. OUTPUT/COLLECTOR

Voltage Traveling Wave Ratio Measurements*

A technique for measuring the mode content of the power flow in a multimode transmission line has been developed. In this section we sketch the analysis behind the measurement technique⁹ and point out some additional experimental considerations.

A. DEFINITION OF VTWR

The ratio of the maximum and minimum values of the beating wave electric fields of any two modes propagating in a multimode guide may, by analogy to the well established vernacular of the single mode waveguide, be denoted the voltage traveling wave ratio (VTWR) for the two modes in question. In general, the VTWR's will be a function of position in the plane normal to the direction of propagation in the guide. Measurements of the VTWR's can be easily related to the fractions of total power propagating in each waveguide mode. This information may be used to:

- (1) characterize the operating mode output of a high power source with multimode output such as a gyrotron,
- (2) analyze the mode conversion properties of overmoded waveguide components,
- (3) determine the optimum locations along the line for lossy obstructions,
- (4) allow transductance matching (induced destructive interference of one or more unwanted modes)¹⁰.

* NOTICE OF IEEE COPYRIGHT: This section contains excerpts from a manuscript which has been accepted for publication in the IEEE Transactions on Microwave Theory and Techniques and is therefore subject to the standard IEEE copyright agreement. This notice is required by that agreement.

The voltage traveling wave ratio (VTWR) is defined in the following manner. Consider the superposition of the two plane waves with complex amplitudes A_n and A_m traveling in a multimode guide in the positive z direction. The resultant wave amplitude may be written as,

$$C(z) = |A_n| e^{ik_n z + i\phi_n} + |A_m| e^{ik_m z + i\phi_m} \quad (1)$$

$$\text{where } \phi_{n,m} \equiv \arctan \left\{ \frac{\text{Im} \langle A_{n,m} \rangle}{\text{Re} \langle A_{n,m} \rangle} \right\} \quad (2)$$

and $k_{n,m}$ are the propagation constants or wave numbers. Cases where such a resultant wave, or beat pattern, is measured by a detector sensitive to the quantity,

$$|C(z)|^2 = |A_n|^2 + |A_m|^2 + 2 |A_n| |A_m| \cos \left\{ (k_n - k_m)z + (\phi_n - \phi_m) \right\}$$

are of interest. The beat wave number is defined as $k_{nm} \equiv (k_n - k_m)/2$. The beat wavelength is $\lambda_{nm} \equiv 2\pi/k_{nm}$. The beat phase, $(\phi_n - \phi_m)$, may be eliminated by suitable choice of origin in z . Solving for the ratio of the maximum and minimum values of $C(z)$ we define the voltage traveling wave ratio,

$$\text{VTWR} \equiv \frac{|C(z)|_{\max}}{|C(z)|_{\min}} = \frac{|A_n| + |A_m|}{|A_n| - |A_m|} = \pm \left(\frac{|A_n| + |A_m|}{|A_n| - |A_m|} \right); \begin{cases} \text{Upper sign:} \\ |A_n| > |A_m|, \\ \text{Lower sign:} \\ |A_n| < |A_m| \end{cases} \quad (4)$$

where the value of the VTWR can range from unity to infinity. This equation can be solved for the ratio

$$\frac{|A_m|^2}{|A_n|^2} = \left(\frac{\text{VTWR} \mp 1}{\text{VTWR} \pm 1} \right)^2 \begin{matrix} \text{Upper Sign} & |A_n| > |A_m| \\ \text{Lower Sign} & |A_n| < |A_m| \end{matrix} \quad (5)$$

Equation (5) relates a measurable quantity, the VTWR for modes n and m , to the ratio of traveling plane wave amplitudes.

B. VTWR'S IN CYLINDRICAL WAVEGUIDE

The fractions $|a_n|^2$ of the total transmission line power contained in each waveguide mode can be deduced from the measured beat wave pattern $|C(\vec{r}, z)|^2$. The multimode transmission line is uniform in the direction of propagation but may have any arbitrary cross section. The measured resultant beat wave pattern arises from the superposition of many modes traveling in the positive z direction. This general case (arbitrary number of modes traveling in a waveguide of arbitrary cross section) has been analyzed and the exact treatment by which $|C(\vec{r}, z)|^2$ may be decomposed into the constituent normal modes of the waveguide can be prescribed.¹¹

For the special case of two circular electric modes propagating in cylindrical waveguide the general result may be simplified. Using the definition (Eq. 4), the mode power ratio can be determined:

$$\frac{|a_m|^2}{|a_n|^2} = G_{nm}(r) \left(\frac{VTWR(r) \mp 1}{VTWR(r) \pm 1} \right)^2 \quad (6)$$

where the guide factor is defined according to:

$$G_{nm}(r) \equiv \frac{\left| J_0(x_m) \right|^2 \left| J_1\left(\frac{x_n r}{a}\right) \right|^2}{\left| J_0(x_n) \right|^2 \left| J_1\left(\frac{x_m r}{a}\right) \right|^2}, \text{ with } G_{nm}(r) = G_{mn}^{-1}(r).$$

C. MODE BUNCHES

When VTWR measurements are performed on systems in which the transductance mismatches are not severe, the general analysis¹¹ may be simplified. One such simplification which is useful in gyrotron engineering is that one need only consider transduction of a pure TE_{on} mode into the mode bunch ($TE_{o\ n-1}$, TE_{on} , $TE_{o\ n+1}$). This approximate treatment is often valid because mode conversion occurs preferentially into nearest neighbor modes¹². (The exception to this occurs when a resonant structure

is encountered, such as a waveguide segment close to a mode cutoff.) Thus a pure TE_{on} circular electric mode will tend to diffuse under an envelope in k -space to form a bunch of modes centered at $k = k_n$ with the wings of the k -space envelope trailing to zero for other modes $m \neq n$. For example, in cylindrical waveguides the TE_{on} mode bunches are contained under the envelope:

$$P_k \propto \frac{X_{1n}^2 X_{1m}^2}{(X_{1n}^2 - X_{1m}^2)^4} \quad (7)$$

where X_{1n} is the n^{th} positive root of $J_1(X) = 0$. For $n \sim 1$, it can be seen from (7) that since $P_k \sim m^{-6}$ the mode bunch is effectively limited to the three modes $m = n-1, n$, and $n+1$.

D. GUIDE FACTORS

The two-mode guide factor, G_{nm} , defined in (6) has been computed for the mode bunches presently of interest in gyrotron research (Table I). The two mode VTWR equation (6) can be used when considering bunches of three modes by performing the VTWR measurements at a radial position for which one of the three modes is identically zero. For example, to find the mode power fractions for the mode bunch ($TE_{01}, TE_{02}, TE_{03}$), the mode power ratios, $|a_2|^2/|a_1|^2$ and $|a_3|^2/|a_1|^2$ must be measured. [The ratio $|a_3|^2/|a_2|^2$ in this unique example is not measured because the TE_{01} has no non-trivial nulls.] This requires the computation of G_{13} and G_{12} . There are often more than one radial null to choose from as shown in Table I. In this case, the values of $G_{13}(X_1 a/X_2) = 1.091$, $G_{12}(X_1 a/X_3) = 0.7961$, and $G_{12}(X_2 a/X_3) = 1.256$ are required.

The VTWR measurements must be performed over a longitudinal interval which is greater than or equal to one-half of the largest beat wavelength, λ_{nm} , of interest in the system. Table II lists all the half beat wavelengths for pairs of circular electric mode through the TE_{05} for the standard 2 1/2" diameter multimode guide at several frequencies. Table III lists the minimum VTWR measurement intervals for the first three circular electric mode bunches. These intervals are on the order of 10" - 20" and

TABLE I

GUIDE FACTOR FOR CIRCULAR ELECTRIC MODE BUNCHES

RADIAL NULL POINTS (r/a)	RADIAL NULL POINTS (inches, in 2.5" DIAM. GUIDE)	MODE BUNCHES									
		TE01,	TE02,	TE03	TE02,	TE03,	TE04	TE03,	TE04,	TE05	
		GUIDE FACTOR			GUIDE FACTOR			GUIDE FACTOR			
NONE	—	G23	—								
$\frac{X_1}{X_2} = 0.5462$	0.683	G13	1.091		G34	15.04					
$\frac{X_1}{X_3} = 0.3766$	0.471	G12	0.7961		G24	1.026	G45	1.633			
$\frac{X_2}{X_3} = 0.6896$	0.862		1.256			1.024					
$\frac{X_1}{X_4} = 0.2876$	0.360				G23	1.709	G35	1.011			
$\frac{X_2}{X_4} = 0.5265$	0.658					0.01832			1.542		
$\frac{X_3}{X_4} = 0.7636$	0.955					2.175			1.010		
$\frac{X_1}{X_5} = 0.2326$	0.291						G34	2.344			
$\frac{X_2}{X_5} = 0.4259$	0.532							0.2382			
$\frac{X_3}{X_5} = 0.6177$	0.772							0.5072			
$\frac{X_4}{X_5} = 0.8089$	1.011							2.729			

TABLE II

ONE-HALF BEAT WAVELENGTHS (INCHES)						
	FREQ. (GHz)	28	35	60	90	110
	FREE SPACE WAVELENGTH (in.)	0.422	0.337	0.197	0.131	0.107
MODE PAIR						
TE ₀₁	TE ₀₂	8.1	10.3	17.9	27.1	33.3
	TE ₀₃	3.0	3.9	6.9	10.5	12.9
	TE ₀₄	1.5	2.0	3.7	5.7	7.0
	TE ₀₅	0.8	1.2	2.3	3.6	4.4
TE ₀₂	TE ₀₃	4.8	6.3	11.3	17.2	21.1
	TE ₀₄	1.9	2.5	4.7	7.2	8.9
	TE ₀₅	0.9	1.4	2.7	4.1	5.1
TE ₀₃	TE ₀₄	3.0	4.3	8.1	12.5	15.4
	TE ₀₅	1.1	1.8	3.5	5.5	6.8
TE ₀₄	TE ₀₅	1.8	3.0	6.2	9.7	12.0

TABLE III

VTWR MEASUREMENT INTERVALS (inches)

FREQUENCY (GHz)	FREE SPACE WAVELENGTH (inches)	MODE BUNCH		
		TE ₀₁ , TE ₀₂ , TE ₀₃	TE ₀₂ , TE ₀₃ , TE ₀₄	TE ₀₃ , TE ₀₄ , TE ₀₅
28	0.422	8.1	4.8	3.0
35	0.337	10.3	6.3	4.3
60	0.197	17.9	11.3	8.1
90	0.131	27.1	17.2	12.5
110	0.107	33.3	21.1	15.4

are not too large for performing practical VTWR measurements. Although the present trend in gyrotron design is toward higher frequency (downward in Table III) this is accompanied by a trend in operating mode toward higher radial mode number (to the right in Table III). Thus for present circular electric mode devices, or those under consideration, the relevant VTWR measurement intervals will remain in the practical range of 10" - 20".

VII. WINDOW

The mechanical design of a single disc beryllia window 1.5λ long was completed this quarter.

All window parts have been received with the exception of some ceramic backing rings, which are due July 18 and the output waveguide flange, being due July 25. Any change in flange design, of course, will affect this date.

Assembly of the first window is not expected to be a gating item.

The computed VSWR for a 1.5λ thick beryllia window is shown by the dashed curve in Figure 4. It is recognized that the limited bandwidth of the window may prove to be a problem in raising the Q of adjacent tube resonances. Efforts are being made to broaden the bandwidth of the window using sophisticated techniques. The computed VSWR for a simulated improved window is shown by the solid curve in Figure 4.

The computed VSWR for an FC-75 face-cooled alumina double disc window is shown in Figure 5. By comparison, the computed VSWR for an FC-75 face-cooled beryllia double-disc window is shown by the dashed curve in Figure 6. The lower dielectric constant of the beryllia results in a wider bandwidth compared to alumina. The computed VSWR of an improved FC-75 face-cooled beryllia double-disc is shown by the solid curve in Figure 6.

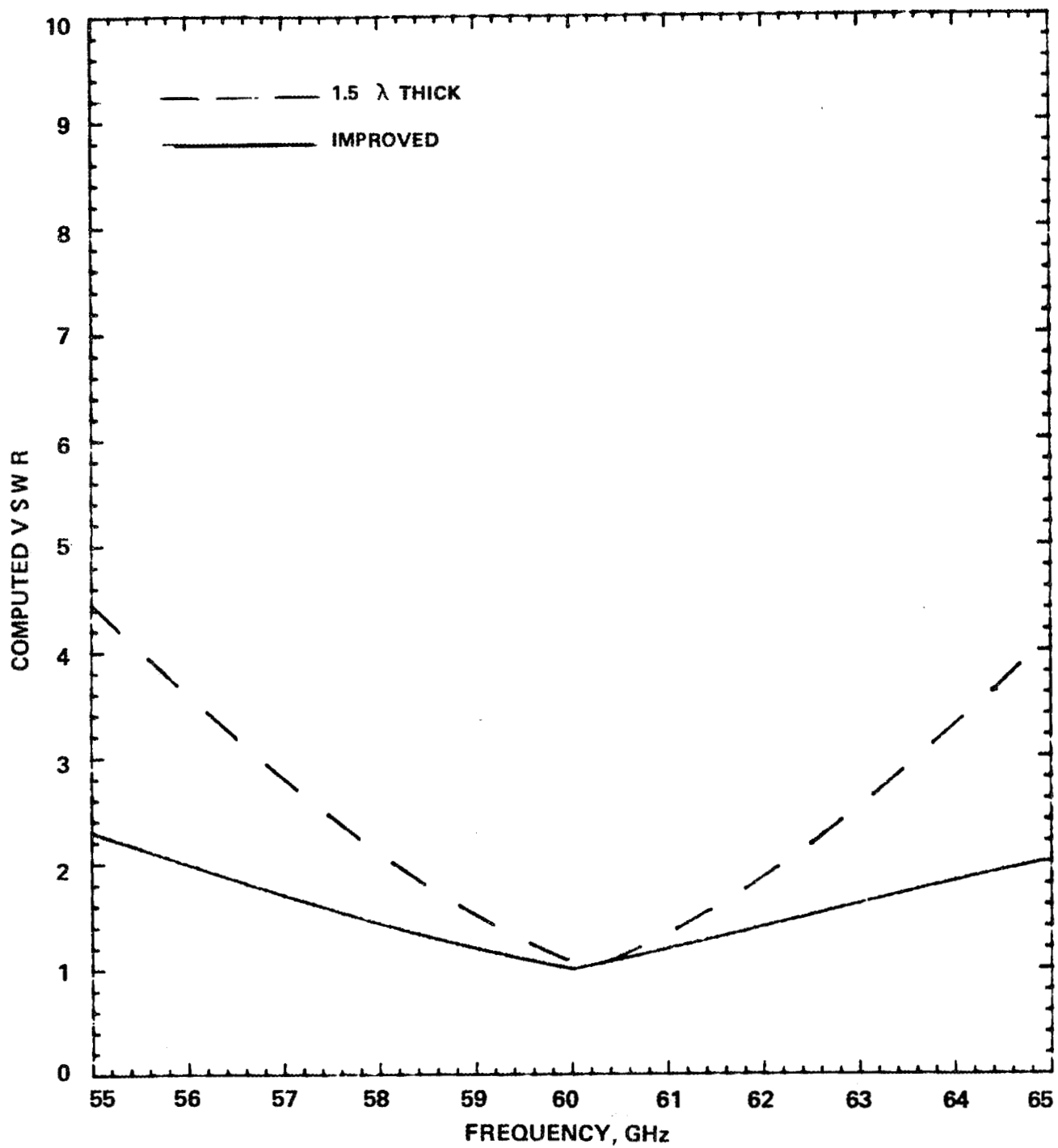


FIGURE 4. COMPUTED VSWR FOR A SINGLE-DISC BERYLLIA WINDOW

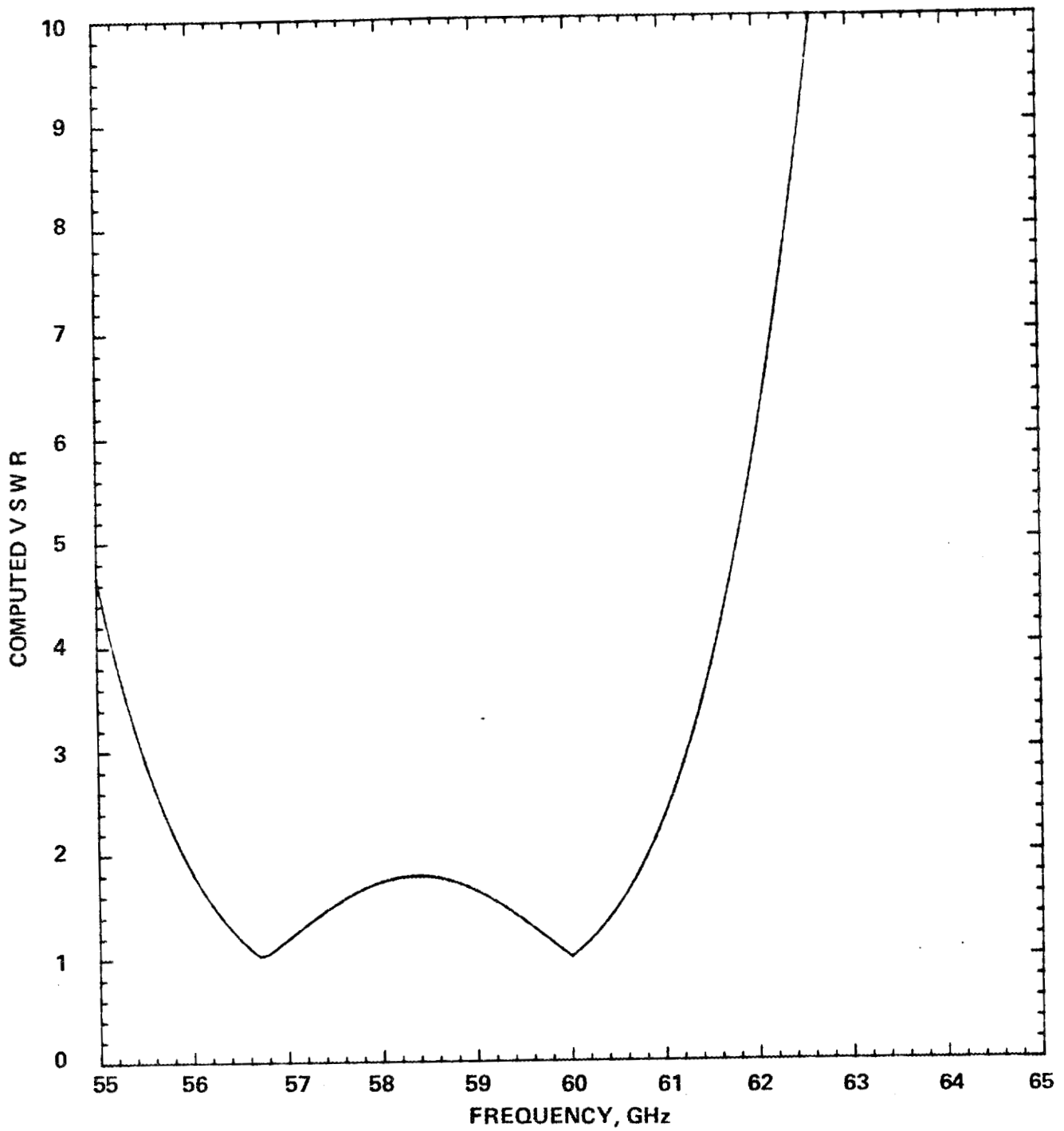


FIGURE 5. COMPUTED VSWR FOR AN FC-75 FACE-COOLED ALUMINA DOUBLE-DISC WINDOW

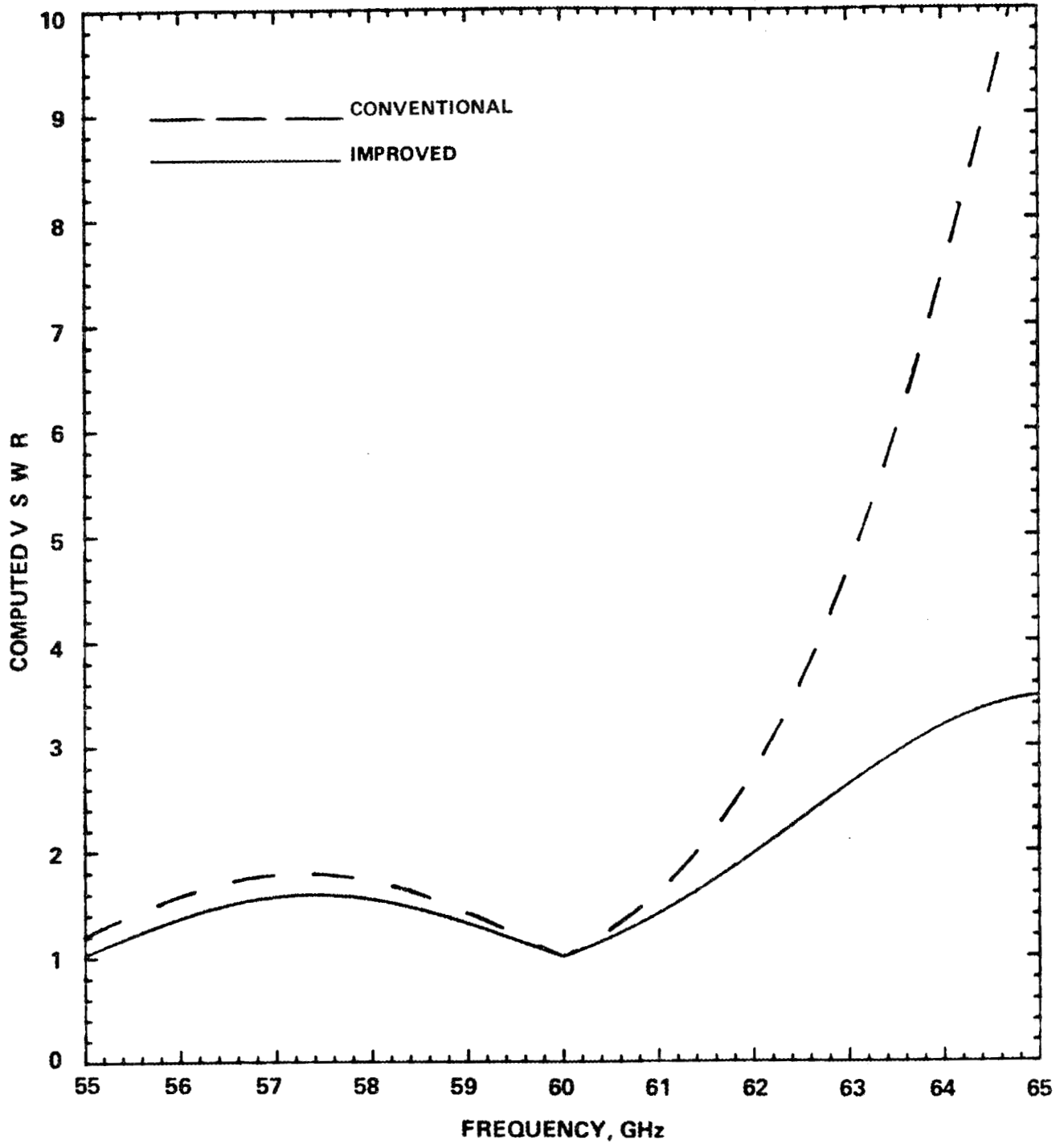


FIGURE 6. COMPUTED VSWR FOR AN-FC-75 FACE-COOLED BERYLLIA DOUBLE-DISC WINDOW

VIII. MECHANICAL DESIGN

The experimental gyrotron consists of several major subassemblies:

1. Single-disc window assembly
2. Collector extension assembly
3. Two collector ceramic assemblies
4. Tubulation assembly
5. Collector assembly
6. VacIon pump assembly
7. Output Taper Assembly
8. Three Elbow Assemblies
9. Body Cylinder Assembly
10. Beam Shaver and Output Assembly
11. Anode Shroud Assembly
12. K-8060 Final Cathode Assembly

These major subassemblies are joined to one another with tungsten inert gas welded joints. This modular construction allows ease of modification and rebuilding. This type of construction is also necessary to reduce the number of braze cycles and to accommodate construction of assemblies too large to fit in the hydrogen braze furnaces.

The K-8060 final cathode assembly is composed of two assemblies, the final cathode stem assembly and the high voltage seal assembly, which are joined at the base of the tube by tungsten inert gas weld. Radial alignment is accomplished by mating cylinders at the base. Axial alignment is assured by a machined step.

The anode shroud assembly comprises several stainless steel body shrouds and a weld ring. It forms the lower portion of the vacuum envelope surrounding the anode and provides structural support between the K-8060 final cathode assembly and the body cylinder assembly.

The beam shaver and output assembly, which is housed within the anode shroud assembly and the body cylinder assembly includes a hydrogen furnace

brazed collection of rf load ring assemblies, the output cavity, the anode assembly and water cooling tubing.

The body cylinder assembly is a welded stainless steel plate and shell assembly which forms the vacuum envelope surrounding the upper portion of the beam shaver and output assembly and the lower portion of the output taper assembly. It also provides structural support between the anode shroud assembly and the output taper assembly.

Three elbow assemblies consisting of a coolant tube brazed to weld adapters provide cooling water to the beam shaver and output assembly and to the lower end of the output taper assembly, all of which are inside the body cylinder assembly.

The output taper assembly is composed of a copper tapered waveguide. It is surrounded by a stainless steel water jacket and a stainless steel plate and shell section at the top that provides structural support between the body cylinder assembly and the lower collector ceramic assembly. The assembly also provides a water pipe for the top of the taper assembly and an elbow to connect to the VacIon pump assembly.

The VacIon pump assembly is comprised of two stainless steel tubulations, a stainless steel manifold and an eight liter per second VacIon pump. The tubulation of this assembly connects to an elbow on the output taper assembly. The purpose of this pumping channel is to pump the cathode region of the tube through the anode shroud, body cylinder and output taper assemblies independent of the beam tunnel.

The collector assembly includes a stack of water cooled copper cylindrical sections with stainless steel plate and shell water manifolds at the top and bottom. Four stainless steel stiffening bars provide structural support between the tube lifting eyes, welded to the top water manifold, and the lower water manifold. The collector assembly provides structural support between the upper and lower collector ceramic assemblies.

The collector ceramic assemblies which are metal and ceramic assemblies are used to isolate the collector electrically to enable monitoring of body, collector and window current. The collector ceramic assemblies provide compressive support between the output taper assembly and collector assembly and also between the collector assembly and collector extension assembly. Tensile support is provided by insulated bolts.

The collector extension assembly consists of a 2.5" inside diameter copper waveguide, water cooled by a stainless steel plate and a shell water jacket. The assembly also includes a stainless steel plate and shell vacuum pumping manifold for evacuation and pumping through the gap between the collector and collector extension assemblies. The plate and shell sections provide structural support between the upper collector ceramic and single-disc window assemblies.

The tubulation assembly includes two sealing rings and a piece of tubulation. The assembly goes between the collector extension assembly and the pumping station during bakeout. After bakeout, part of this assembly is pinched off.

The single-disc window assembly is composed of:

1. The beryllia window disc;
2. a short waveguide section on the vacuum side ending in a copper cup for the window braze;
3. a short waveguide section on the air side with a copper cup on one end for the window braze;
4. a stainless steel waveguide flange, terminating the tube, and
5. a plate and shell water jacket providing structural support for the window waveguide.

IX. COMPONENTS

Design work is continuing on the 60 GHz waveguide components. The high power 60 GHz mode filter will be similar to the 28 GHz mode filter in mechanical design. The electromagnetic properties of the design will be examined in cold test and mode filter cold test parts are on order. Analytical work on the mode filter design and on the behavior of mode filters when they are combined with other waveguide components, such as miter bends, has begun. The electromagnetic design of the power sampler/arc detector has been specified and mechanical design is underway.

X. TUBE ASSEMBLY

Seventy-six percent of the piece parts for the first experimental tube have been received. The last of the piece parts are expected August 8, 1980.

The last of the gun parts are expected in mid-July at which time construction of the electron gun will start. The first completed gun is expected in August.

Ninety-one percent of the interaction circuit assembly piece parts have been received and assembly has been started.

Sixty-five percent of the output/collector assembly piece parts have been received. The last parts are due July 23.

Sixty-two percent of the window parts have been received. The remaining parts are due August 8.

XI. PROGRAM SCHEDULE AND PLANS

Parts are being received and the construction of the first experimental 60 GHz gyrotron, serial number X-1, has been started.

Completion of the first electron gun is expected during the next quarter.

A superconducting magnet design review meeting will be held July 18 at Magnetic Corporation of America. Progress during the next quarter will include completion of the design and fabrication of the conductor.

Parts are being received for the pulsed oscillator interaction circuit. During the next quarter the circuit assembly will be assembled. Parallel cold test work will continue.

All of the output window parts should be received during the next quarter.

The final assembly drawings will be completed during the next quarter for both the experimental pulsed gyrotron and the 100 ms pulse duration gyrotron.

All piece parts for the experimental and first 100 ms pulse duration gyrotrons are expected to be delivered during the next quarter.

Construction of the waveguide components, pulsed waterload and power sampler and arc detector will be started during the next quarter.

Test set modification will continue during the next quarter. Completion of the short pulse modification is not expected before the beginning of January.

The milestone chart and status report is shown in Figure 7.

MILESTONE CHART AND STATUS REPORT

○ ORIGINAL START □ REVISED START △ MAJOR MILESTONE
 ▽ INTERMEDIATE OR DECISION POINT ◇ PROPOSED SCHEDULED DEVIATION FOR A MAJOR MILESTONE
 ↓ STATUS REPORT TIME — ACTIVITY SCHEDULED — ACTIVITY COMPLETED

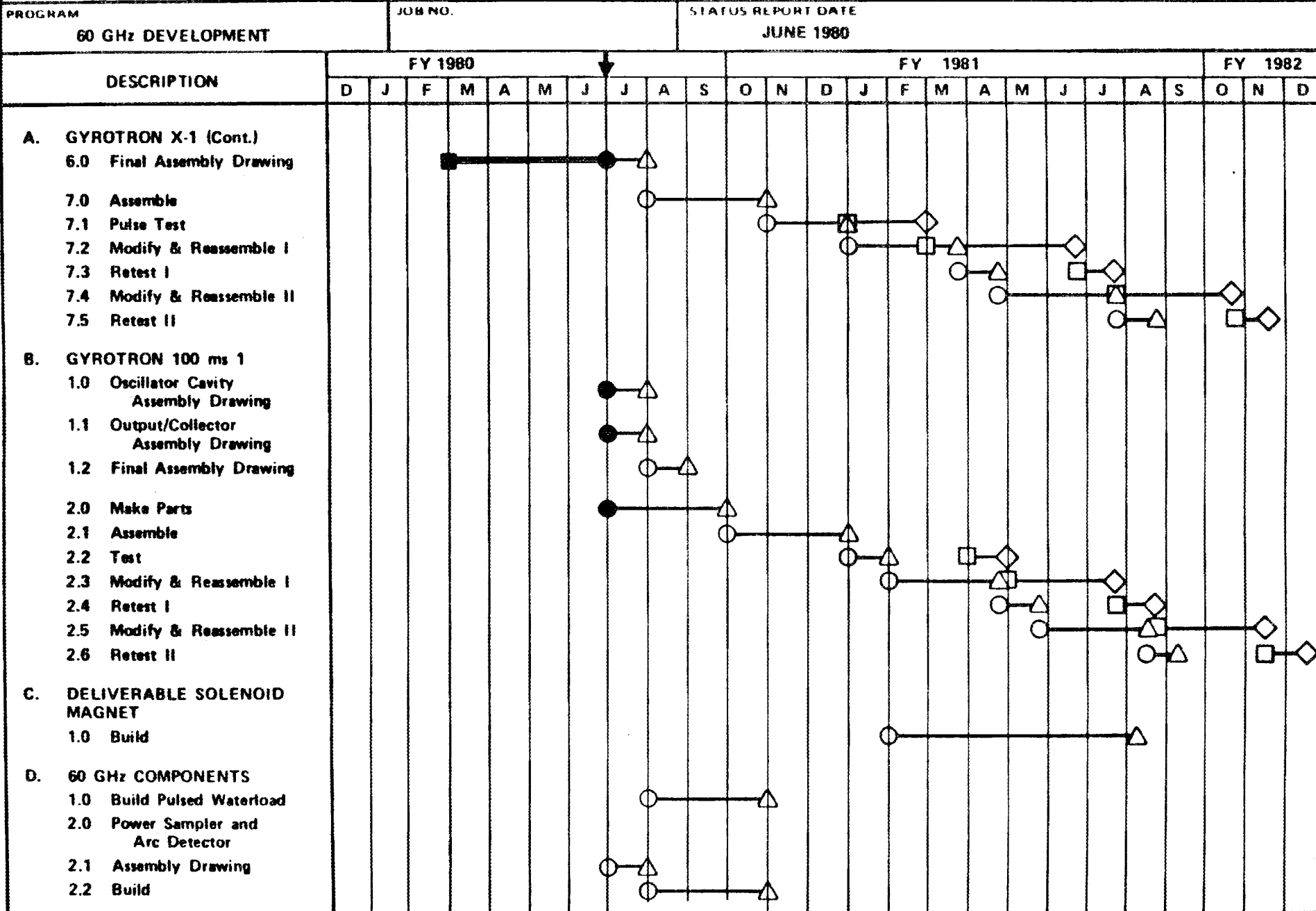


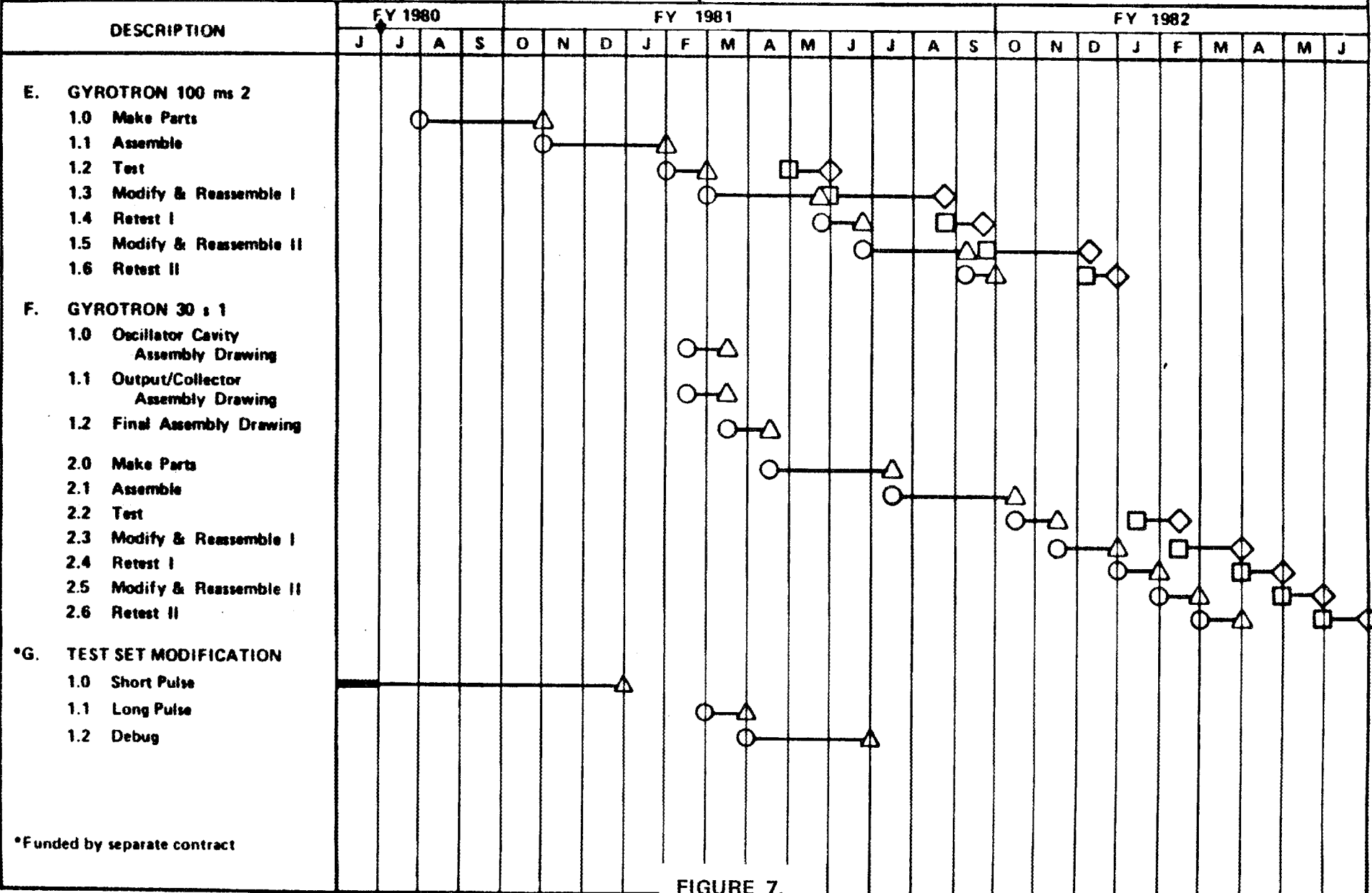
FIGURE 7.

31

MILESTONE CHART AND STATUS REPORT

○ ORIGINAL START □ REVISED START △ MAJOR MILESTONE
 ▽ INTERMEDIATE OR DECISION POINT ◇ PROPOSED SCHEDULED DEVIATION FOR A MAJOR MILESTONE
 ↓ STATUS REPORT TIME — ACTIVITY SCHEDULED — ACTIVITY COMPLETED

PROGRAM: **60 GHz DEVELOPMENT** JOB NO.: _____ STATUS REPORT DATE: **JUNE 1980**



*Funded by separate contract

FIGURE 7.

32

MILESTONE CHART AND STATUS REPORT

○ ORIGINAL START □ REVISED START △ MAJOR MILESTONE
 ▽ INTERMEDIATE OR DECISION POINT ◇ PROPOSED SCHEDULED DEVIATION FOR A MAJOR MILESTONE
 ↓ STATUS REPORT TIME — ACTIVITY SCHEDULED — ACTIVITY COMPLETED

PROGRAM: 60 GHz DEVELOPMENT JOB NO.: STATUS REPORT DATE: JUNE 1980

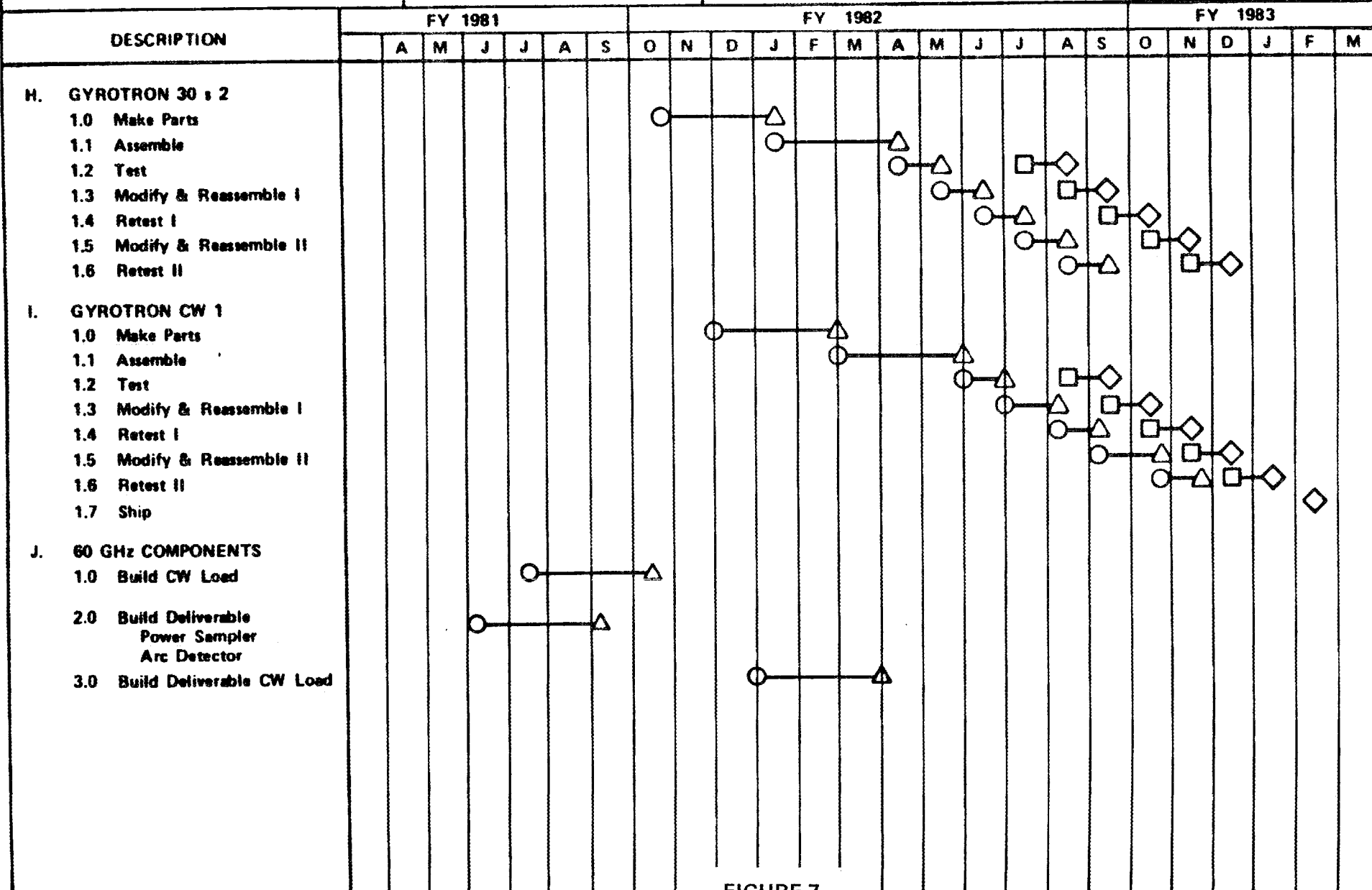


FIGURE 7

33

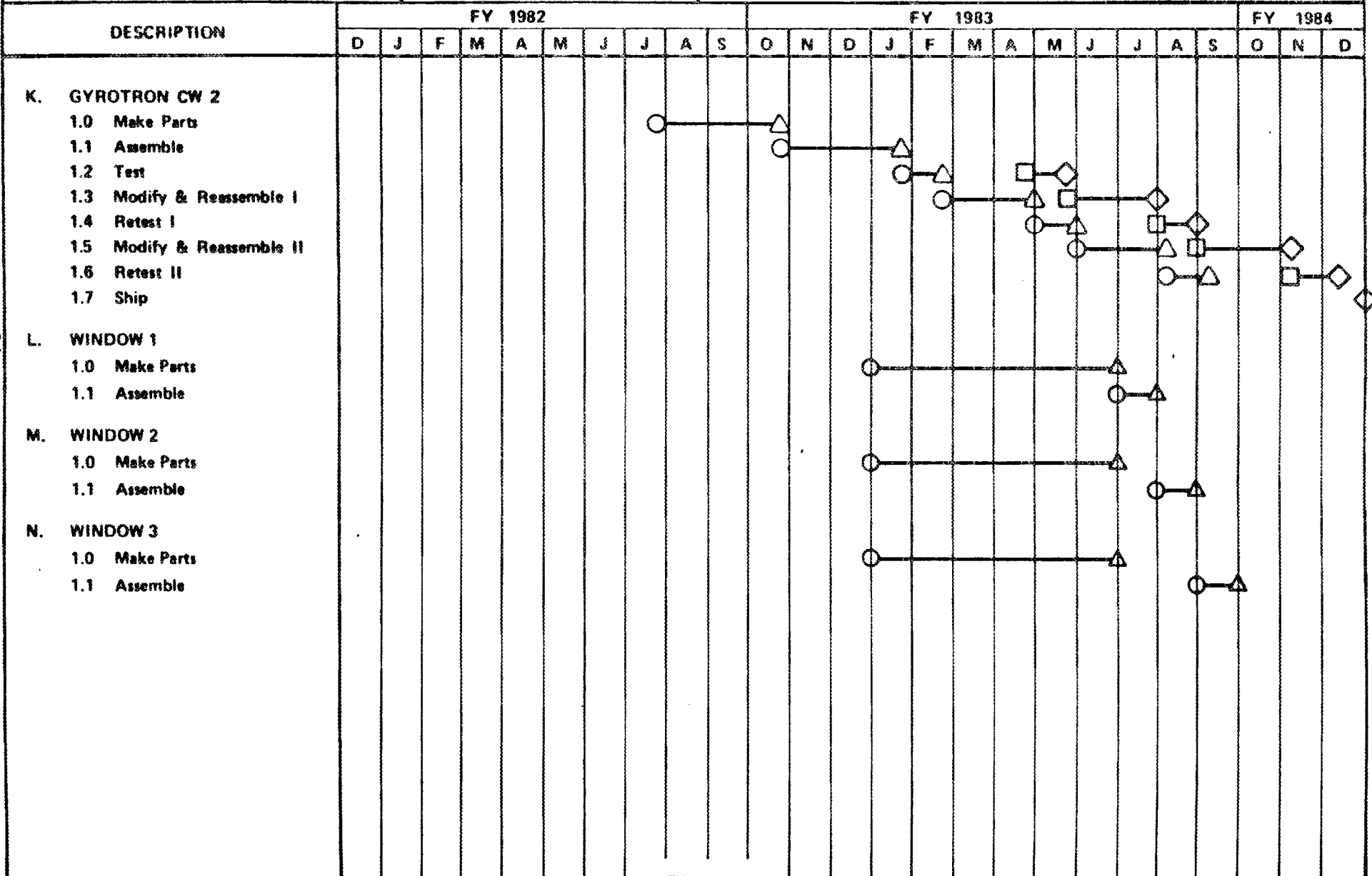
MILESTONE CHART AND STATUS REPORT

○ ORIGINAL START □ REVISED START △ MAJOR MILESTONE
 ▽ INTERMEDIATE OR DECISION POINT ◇ PROPOSED SCHEDULED DEVIATION FOR A MAJOR MILESTONE
 ↓ STATUS REPORT TIME — ACTIVITY SCHEDULED — ACTIVITY COMPLETED

PROGRAM
60 GHz DEVELOPMENT

JOB NO.

STATUS REPORT DATE
JUNE 1980



34

XII. REFERENCES

1. H.R. Jory, E.L. Lien and R.S. Symons, Final Report, "Millimeter Wave Study Program," Oak Ridge National Laboratory Order No. Y12 11Y-49438 V, Varian Associates, Inc., November 1975.
2. D.V. Kisel, G.S. Korablev, V.G. Naval' yev, M.I. Petelin and Sh. E. Tsimring, "An Experimental Study of a Gyrotron, Operating at the Second Harmonic of the Cyclotron Frequency, with Optimized Distribution of the High Frequency Field," Radio Engineering and Electronic Physics, Vol. 19, No. 4, 95 - 100, 1974.
3. S. Hegji, H. Jory and J. Shively, "Development Program for a 200 kW CW, 28 GHz Gyroklystron" Quarterly Report No. 6, Union Carbide Corporation Contract No. 53X01617C, Varian Associates, Inc., July through September 1977.
4. H. Jory, S. Evans, S. Hegji, J. Shively, R. Symons and N. Taylor "Development Program for a 200 kW, CW 28 GHz Gyroklystron Quarterly Report No. 9", Union Carbide Corporation Contract No. W-7405-eng-26, ORNL Sub-01617/9, Varian Associates, Inc., April through June 1978.
5. V.A. Flyagin et al, "The Gyrotron", IEEE Trans. MTT-25, No. 6 pp. 522-527, June 1977.
6. J.F. Shively et al, "Recent Advances in Gyrotrons," 1980 IEEE MTT-S International Microwave Symposium Digest, 28-30 May 1980, Washington, D.C., IEEE Catalog No. 80CH1545-3 MTT, pp 99-101.
7. F. Friedlander, E. Galli, H. Jory, F. Kinney, K. Miller, J. Shively and R. Symons, "Development Program for a 200 kW, CW 28 GHz Gyroklystron Quarterly Report No. 1" Union Carbide Corporation Contract No. 53X01617C, Varian Associates, Inc., October 1976.

8. F. Friedlander, E. Galli, H. Jory, K. Miller, J. Shively and R. Symons, "Development Program for a 200 kW, CW 28 GHz Gyroklystron Quarterly Report No. 2" Union Carbide Corporation Contract No. 53X01617C, Varian Associates, Inc., October 1976.
9. D. S. Stone, "Mode Analysis in multimode waveguides using voltage traveling wave ratios," IEEE-MTT to be published; D.S. Stone, "Measurement of Voltage Traveling Wave Ratios in Multimode Transmission Lines," Bull. Am. Phys. Soc., October 1980.
10. The concept of transductance matching in multimode waveguides has been described by L. Solymar, "Monotonic Multi-Section Tapers for Overmoded Circular Waveguides", IEE paper No. 2839R, pp. 121-128, January 1959.
11. See Section III of reference 9.
12. J.F. Shively, D.S. Stone, and G.E. Wendell, "60 GHz Gyrotron Development Program", Quarterly Report No. 3, Union Carbide Corporation Contract No. W-7405-eng-26, ORNL Sub-01617/9, Varian Associates, Inc., January through March 1980, p. 16.

INTERNAL DISTRIBUTION

1. L.A. Berry
2. A.L. Boch
3. J.L. Burke
4. R.J. Colchin
- 5-8. H.O. Eason
9. O.C. Eldridge
10. R.P. Jernigan
- 11-13. C.M. Loring
14. H.C. McCurdy
15. O.B. Morgan, Jr.
16. G.F. Pierce
17. T.L. White
- 18-19. Laboratory Records Department
20. Laboratory Records, ORNL-RC
21. Y-12 Document Reference Section
- 22-23. Central Research Library
24. Fusion Energy Division Library
25. Fusion Energy Division Communications Center
26. ORNL Patent Office

EXTERNAL DISTRIBUTION

27. R.A. Dandl, 1122 Calle De Los Serranos, San Marcos, CA 92069
28. R.J. DeBellis, McDonnell Douglas Astronautics Co., P.O. Box 516,
St. Louis, MO 63166
29. A.N. Dellis, Culham Laboratory, Abingdon, Oxon, England, OX143DB
30. W.P. Ernst, Princeton University, Plasma Physics Laboratory, P.O.
Box 451, Princeton, NJ 08540
31. W. Friz, AFAL/DHM, Wright Patterson AFB, OH 45433
32. T. Godlove, Particle Beam Program, Office of Inertial Fusion,
Department of Energy, Mail Stop C-404, Washington, DC 20545
33. V.L. Granatstein, Naval Research Laboratory, Code 6740, Washington,
DC 20375

34. G.M. Haas, Component Development Branch, Office of Fusion Energy (ETM), Department of Energy, Mail Stop G-234, Washington, DC 20545
35. J.L. Hirshfield, Yale University, Department of Engineering and Applied Science, P.O. Box 2159, Yale Station, New Haven, CT 06520
36. H. Ikegami, Institute of Plasma Physics, Nagoya University, Nagoya 464, Japan
37. J.V. Lebacqz, Stanford Linear Accelerator Center, P.O. Box 4349, Stanford, CA 94305
38. W. Lindquist, Electronics Engineering Department, Lawrence Livermore Laboratory, P.O. Box 808/L-443, Livermore, CA 94550
39. K.G. Moses, TRW Defense and Space Systems, 1 Space Park, Bldg R-1, Redondo Beach, CA 90278
40. M.R. Murphy, Office of Fusion Energy (ETM), Department of Energy, Mail Stop G-234, Washington, DC 20545
41. V.B. Napper, Three Dunwoody Park, Suite 112, Atlanta, GA 30341
42. B.H. Quon, TRW Defense and Space Systems, 1 Space Park, Bldg R-1, Redondo Beach, CA 90278
43. M.E. Read, Naval Research Laboratory, Code 6740, Washington, DC 20375
44. D.B. Remsen, General Atomic Company, P.O. Box 81608, San Diego, CA 92138
45. B. Stallard, Lawrence Livermore Laboratory, University of California, L-437, P.O. Box 808, Livermore, CA 94550
46. H.S. Staten, Office of Fusion Energy (ETM), Department of Energy, Mail Stop G-234, Washington, DC 20545
47. P. Tallerico, AT-1, Accelerator Technology Division, Los Alamos Scientific Laboratory, Mail Stop 817, P.O. Box 1663, Los Alamos, NM 87545
48. J.J. Tancredi, Hughes Aircraft Company, Electron Dynamics Division, 3100 W. Lomita Blvd., Torrance, CA 90509
49. R.J. Temkin, National Magnet Laboratory, Massachusetts Institute of Technology, Cambridge, MA 02139
50. A. Trivelpiece, Science Applications, Inc., 1200 Prospect Street, P.O. Box 2351, LaJolla, CA 92038
51. Director, U.S. Army Ballistic Missile Defense Advance Technology Center, Attn: D. Schenk, ATC-R, P.O. Box 1500, Huntsville, AL 35807

- 52-53. Department of Energy Technical Information Center, Oak Ridge, TN
37830
54. RADC/OCTP, Griffiss AFB, NY 13441
55. Office of Assistant Manager for Energy Research and Development, Oak
Ridge Operations Office, Department of Energy, Oak Ridge, TN 37830.

VARIAN DISTRIBUTION

56. R. Berry
57. C. Conner
58. S. Evans
59. P. Ferguson
60. T.J. Grant
61. G. Jacobson
62. H. Jory
63. J. Moran
- 64-71. J. Shively
72. A. Staprans
73. D. Stone
74. G. Wendell
- 75-77. R. West